Scaling behavior and negative gain of NAPD

X. Guo[1,2], S. G. Ma[1], X. Y. Zheng[1,3], K. L. Wang[1]

1 Department of Electrical Engineering, University of California, Los Angeles, CA 90095
2 Beijing Optoelectronic Technology Lab, Beijing University of Technology, Beijing, 100022 China
3 Jet Propulsion Laboratory, California Institute of Technology, Pasadena, CA 91109

Abstract

The size-dependent and lamination-dependent I-V curves of nano-multiplication-region avalanche photodiode (NAPD) were measured with the sized of 100nm, 200nm, 1μm, and 10μm. The gain increases with the decrease of the multiplication-region size and illumination power. These data indicate the NAPD possesses the advantages of high gain and high sensitivity. Negative gain was also found in this experiment.

Key words: APD, negative gain, high-gain, high-sensitivity

Introduction

High-performance silicon single-photon avalanche photodiodes (APDs), also called Geiger mode APDs, working in the wavelength $\lambda<1100$ nm due to the bandgap of Si have been available for years. Recently, photodetectors based on AlGaN or SiC realized in the solar-blind operation. However, in order to compete with the existing photomultiplier tube (PMT) effectively, the performance of APDs still has to improve. For applications, PMTs, which require high voltage and large room, have limitations. Compared with semiconductor APDs, they are applied in quantum cryptography, time-resolve spectroscopy, and missile detection, recently.

In this paper, nano-multiplication-region avalanche photodiodes (NAPD) were proposed, which possessed advantages of high gain and high sensitivity. The dark and illuminated I-V curves of NAPDs with four multiplication-region (MR) diameters were measured. The photocurrent gain of NAPDs increases with the decrease of MR diameters, as well as illumination power, which proves the potential for the advantages of NAPDs. The negative differential gain was also observed in this study.

Experimental

Fig. 1 shows the schematic structure of Si-based NAPD. It is basically composed of a bulk absorption region and a nano-size MR, which is defined by inductively coupled plasma etching after E-beam lithography. The diameters of these nano-size MRs in this study are 100 nm, 200 nm, 1 μm and 10 μm, respectively, with the height of about 1 μm. The actual implantation density and the depth from the top surface for the p-type charge layer and the n^{++}-type electron collection layer are about 1×10^{13} cm^{-3}, 0.5μm and 1×10^{18} cm^{-3}, 0.1μm, respectively. The surface of the etched nano-size MR was then passivated by putting the sample to thermal oxidation furnace to reduce the carrier loss and scattering.

To avoid current heating, pulse mode (on time 0.5ms with occupation ratio of 0.25‰) was applied to characterize the I-V behavior for these NAPDs both at room temperature (RT) and 77K. The temperature coefficients α of breakdown voltage V_B, which depends strongly on temperature, are 3.24 mV/K, 3.24 mV/K, 3.7 mV/K, and 4.17 mV/K for the MR diameters of 100 nm, 200 nm, 1 μm and 10 μm, respectively. The close distribution of α proves that the current heating is not important and will not be considered in this study. 488nm laser light was used as illumination source for the NAPDs which was radiating on a single device after some reflective mirrors and lens. After calculation, the illumination powers used in this experiment were about 6 μW, 20 μW, 60 μW, 100 μW, 160 μW and 200 μW, respectively. Keithley 4200 was used for measuring current-voltage (I-V) curves.

Nanoengineering: Fabrication, Properties, Optics, and Devices V, edited by Elizabeth A. Dobisz, Louay A. Eldada, Proc. of SPIE Vol. 7039, 70390N, (2008) · 0277-786X/08/$18 · doi: 10.1117/12.795173

Downloaded from SPIE Digital Library on 15 Nov 2009 to 159.226.100.225. Terms of Use: http://spiedl.org/terms

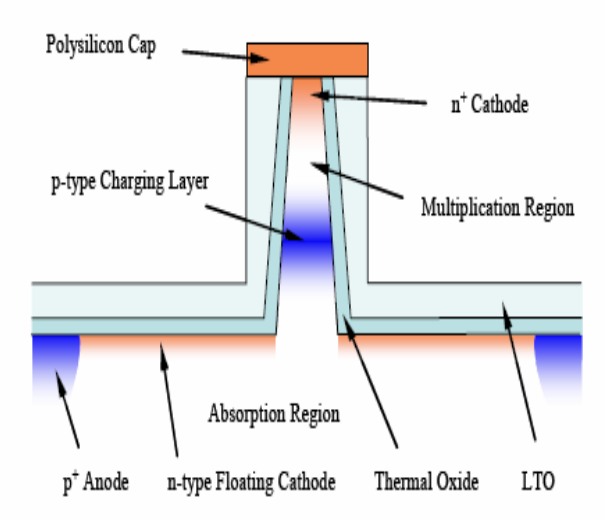

Fig. 1 the designed structure of NAPDs, which is basically composed of a bulk absorption region and a nano-size multiplication-region. The thermal oxide layer was used to reduce carrier loss and scatter at the etched surface.

Results and Discussion

All the I-V curves showed typical avalanche processes. When the applied voltage is above the breakdown voltage, V_B, the current increases sharply. The measured V_B's increased from 7.8V to 9.3V with decreasing the MR diameter. Fig 2 (a) showed the dark I-V curves at room temperature for the NAPDs with the MR sizes of 100 nm, 200 nm, 1 μm, and 10 μm, respectively. Fig. 2 (b) shows a group of I-V curves under the illumination powers of 6 μW, 20 μW, 60 μW, 100 μW, 160 μW and 200 μW, respectively, for the multiplication-region size of 100nm NAPD at room temperature. $V_B' = IR + V_B$, where R is the series resistance in the device and measurement circuit, and V_B' is the measured breakdown voltage, which depends strictly on the doping density and MR's thickness according to $V_B = \frac{E_m W}{2}$, where E_m is the maximum field, W is the depletion width. The difference of V_B's is caused by different pillar size. After about 0.3V above V_B with the increase slop of 45.5μA/V, the current which looks like saturate in log-log scale plot is because of space-charge effect and large space-charge resistance R_{SC} which will be dominant after breakdown. The R_{SC} s and current densities J with ΔV_B of 4V are 38081 Ohm, 32982 Ohm, 22577 Ohm, 14479 Ohm, and 3.83 mA/ μm^2, 3.66 mA/ μm^2, 0.224 mA/ μm^2, 3.67447 μA/ μm^2 for the MR diameters of 100 nm, 200 nm, 1 μm and 10 μm, respectively, where ΔV_B is an extra voltage above the V_B. The saturation current occurred earlier for smaller MR size is still because of their larger R_{SC}.

Downloaded from SPIE Digital Library on 15 Nov 2009 to 159.226.100.225. Terms of Use: http://spiedl.org/terms

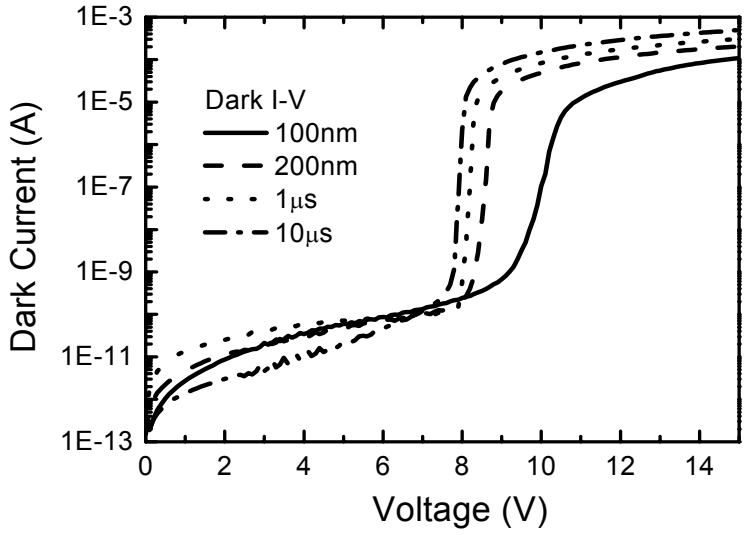

Fig. 2 (a) the dark I-V curves at room temperature for the NAPDs with the MR sizes of 100 nm, 200 nm, 1 μm, and 10 μm, respectively. The measured breakdown voltage increased from 7.8V to 9.3V with decreasing the MR diameter.

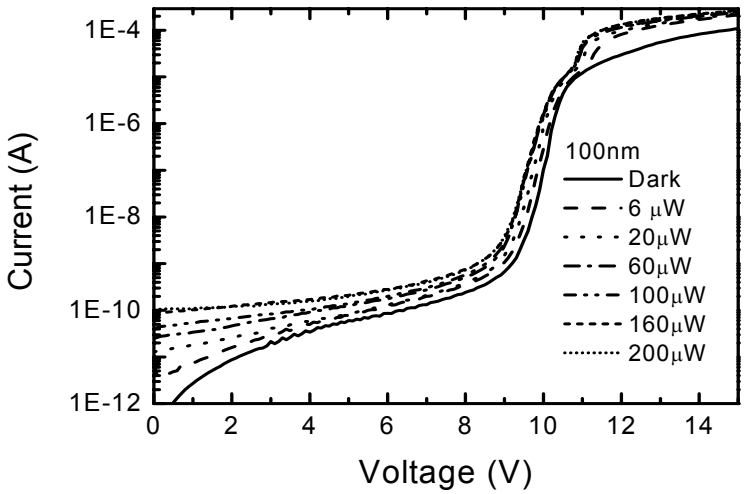

Fig. 2 (b) a group of I-V curves under the illumination powers of 6 μW, 20 μW, 60 μW, 100 μW, 160 μW and 200 μW, respectively, for the multiplication-region size of 100nm NAPD at room temperature.

Downloaded from SPIE Digital Library on 15 Nov 2009 to 159.226.100.225. Terms of Use: http://spiedl.org/terms

The avalanche gain, also called multiplication factor, can be defined as $gain \equiv \frac{(I_{illumination,12V} - I_{dark,12V})}{(I_{illumination,6V} - I_{dark,6V})}$. Here, 6 V and 12 V were selected as two reference voltages before and after breakdown voltage according to our actual measurement results. Fig. 3 showed the avalanche gain dependence on the MR size under the different illumination power after the extraction and calculation from the original dark and illuminated I-V data at room temperature. The avalanche gain ranges from the magnitude of 10^3 to 10^6. According to the data fitting result, the avalanche gain increases exponentially with the decrease of MR size. This result indicates that the NAPDs have the capability of high-sensitivity of detecting smaller signals with decreased multiplication region size, compared with conventional APDs.

Fig. 4 showed the avalanche gain dependence on the multiplication-region sizes with the sizes of 100 nm, 200 nm, 1 μm, and 10 μm, respectively in log-log scale. Also, the gain increases exponentially with the decrease of the size of MR size. Because for the size of 100μm, it can be compared with the commercial APD's MR, or bulk multiplication region, the fact that the avalanche gain increases with the decreasing MR sizes indicates the gain of such NAPDs are higher than conventional APDs.

By now, the advantages of high gain and high sensitivity of NAPDs were demonstrated. The highest gain we obtained was at the magnitude of about 10^6, which is much higher than commercial APDs now. The highest quantum efficiency we obtained in such NAPDs could reach to about 3000.

Fig. 5 showed a family of typical avalanche gain results for such NAPDs under the illumination power of 60 μW. After the breakdown voltage V_B, the gain increases sharply due to avalanche. The obvious negative gain was found in all curves. The negative gain just after the V_B is perhaps caused by the field-induced inter-valley scattering from the conduction-band minimum to the energetically higher, low-mobility valley. The drop of the gain in the negative gain part is strongly depending on the MR size.

When extracted the data of gain peak and valley where the negative gain occurred and plotted in Fig. 6 for the NAPD with the MR size of 10 μm under the illumination power of 6 μW, 20 μW, 60 μW, 100 μW, 160 μW and 200 μW, respectively, we found the avalanche gain peak valley ratio decreased with the illumination power exponentially according to the fitting results, which was shown as dash line in Fig. 6. We still attributed this fact to the field-induced inter-valley scattering from energy lower valley to energy higher, but lower mobility valley. Here, from Fig. 5 and Fig. 6, it is also easy to understand that for the NAPDs with smaller MR size, it is difficult for the negative gain to happen because the effective electric field applied on the smaller NAPDs' multiplication region is lower than that of larger multiplication region NAPDs.

Conclusion

In summary, the advantages of NAPDs of high gain and high sensitivity were demonstrated in this experiment. The gain increases with the decrease of the multiplication-region size and illumination power. The highest gain we obtained in this experiment reached to the magnitude of about 10^6. Also the negative gain was found in such NAPDs. The avalanche gain peak valley ratio also decreased with the illumination power. The physics in NAPDs is the narrowed the multiplication region, which then lowered the effective electric field applied on it, improves the performance of NAPDs a lot.

Acknowledgement

All the authors would like to thank students in DRL group of UCLA for their useful discussion and technical supports.

Downloaded from SPIE Digital Library on 15 Nov 2009 to 159.226.100.225. Terms of Use: http://spiedl.org/terms

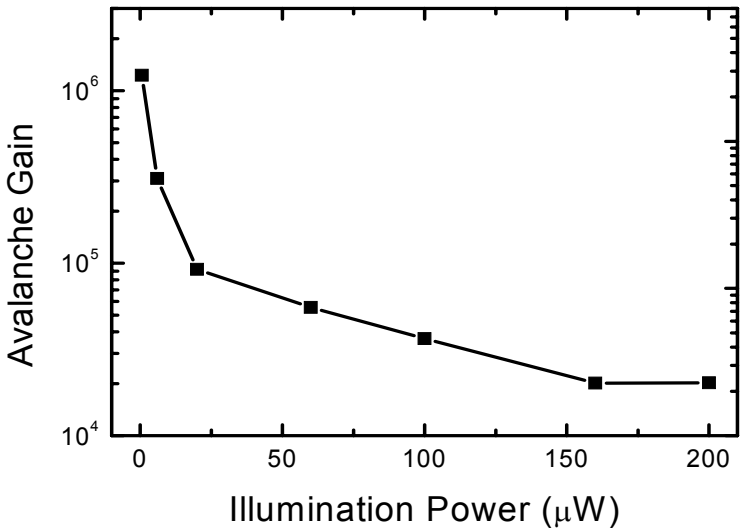

Fig. 3 The dependence of avalanche gain of NAPDs on the illumination powers of 0.6 μW, 6 μW, 20 μW, 60 μW, 100 μW, 160 μW and 200 μW, respectively. The avalanche gain decreases with the illumination power, which indicates the NAPDs have the capability of high-sensitivity for smaller signal compared with conventional APDs.

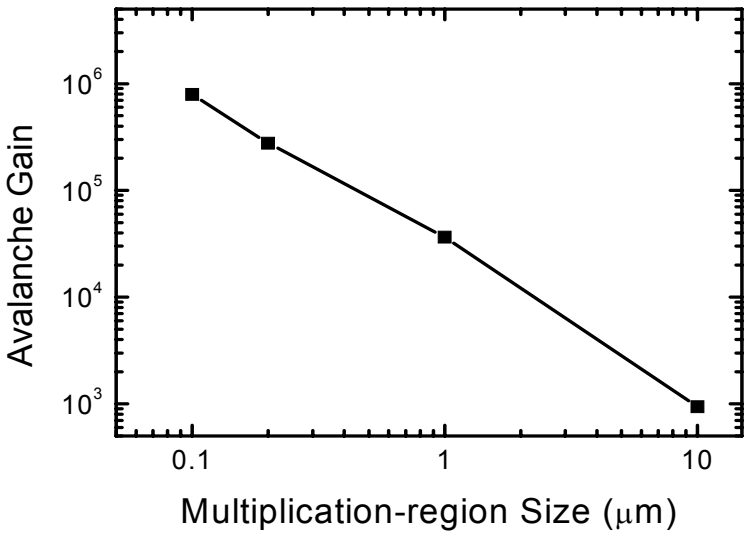

Fig.4 The dependence of avalanche gain on the multiplication-region size of NAPDs with the sizes of of 100 nm, 200 nm, 1 μm, and 10 μm, respectively. The illumination power is 100 μW. The avalanche gain decreases with the multiplication-region size, which indicates the gain of NAPDs is higher than that of conventional APDs under the same illumination level.

Downloaded from SPIE Digital Library on 15 Nov 2009 to 159.226.100.225. Terms of Use: http://spiedl.org/terms

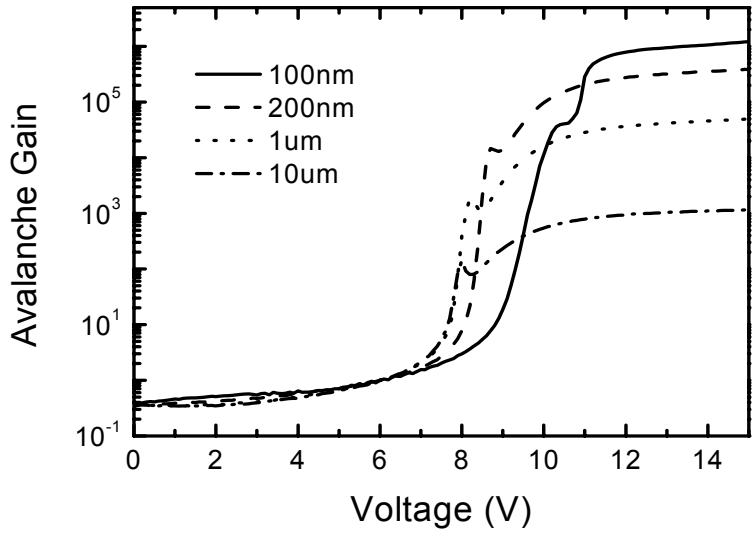

Fig. 5 A family of typical avalanche gain curves for NAPDs under the illumination power of 60 μW for the multiplication-region sizes of 100 nm, 200 nm, 1 μm and 10 μm, respectively.

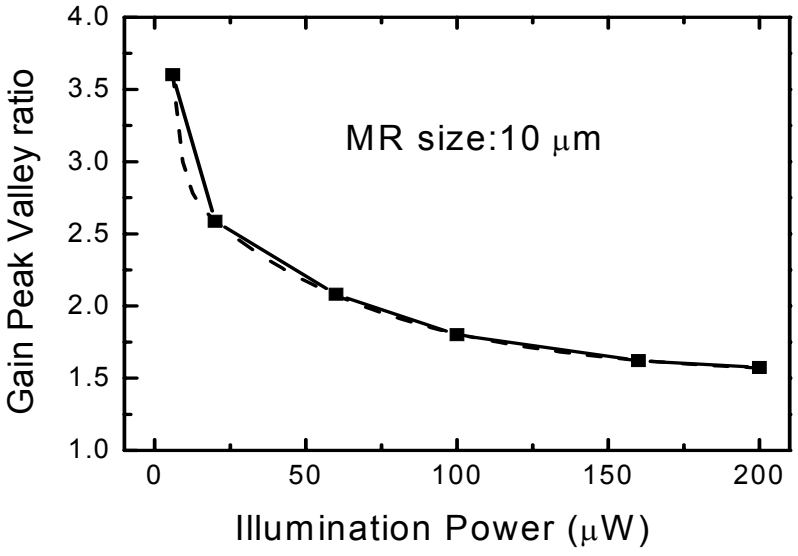

Fig. 6 The avalanche gain peak valley ratio for the MAPD with the multiplication-region size of 10 μm under the illumination power of 6 μW, 20 μW, 60 μW, 100 μW, 160 μW and 200 μW, respectively. The dash line was the fitting result for the gain peak valley ratio data by decreased exponentially with the illumination power.

Downloaded from SPIE Digital Library on 15 Nov 2009 to 159.226.100.225. Terms of Use: http://spiedl.org/terms

References:

[1] O. Marinov, M. J. Deen, and J. A. J. Tejada, "Theory of microplasma fluctuations and noise in silicon diode in avalanche breakdown", J. Appl. Phys., 101(6), 064515-1-20 (2007)

[2] R. J. McINTYRE, "The distribution of gains in uniformly multiplying avalanche photodiodes: Theory", IEEE Transactions on Electron Devices, 19(6), 703-713, (1972)

[3] A. Spinelli, and A. L. Lacaita, "Physics and numerical simulation of single photon avalanche diodes", IEEE Transactions on Electron Devices, 44(11), 1931-1943, (1997)

[4] R. J. McINTYRE, "Theory of microplasma instability in Silicon", J. Appl. Phys., 32(6), 983-995, (1961)

[5] R. Kuvas and C. A. Lee, "Quasistatic approximation for semiconductor avalanches", J. Appl. Phys., 41(4), 1743-1755, (1970)

[6] H. S. Kang, M. J. Lee and W. Y. Choi, "Si avalanche photodetectors fabricated in standard complementary metal-oxide-semiconductor process", Appl. Phys. Lett., 90(15), 151118-1-3, (2007)

[7] R. H. Haitz, "Model for the electrical behavior of a microplasma", J. of Appl. Phys., 35(5), 1370-1376, (1964)

[8] X. Y. Guo, A. L. Beck, X. W. Li, J. C. Campbell, D. Emerson, and J. Sumakeris, "Study of reverse dark current in 4H-SiC avalanche photodiodes", IEEE J. of Quantum Electronics, 41(4), 562-567, (2005)

[9] M. G. Liu, X. G. Bai, C. Hu, X. Y. Guo, J. C. Campbell, Z. Pan, M. M. Tashima, "Low dark count rate and high-single-photon detection efficiency avalanche photodiode in Geiger-mode operation", IEEE Photonics technology Lett., 19(6), 378-380, (2007)

[10] R. McClintock, A. Yasan, K. Minder, P. Kung, and M. Razeghi, "Avalanche multiplication in AlGaN based solar-blind photodetectors", Appl. Phys. Lett., 87, 241123-1-3, (2005)

Downloaded from SPIE Digital Library on 15 Nov 2009 to 159.226.100.225. Terms of Use: http://spiedl.org/terms